Scientia Iranica (2025) **32**(18): 8476

Sharif University of Technology
Scientia Iranica
Transactions on Nanotechnology
https://scientiairanica.sharif.edu

Thermal applications of hybrid nanofluid containing carbon nanotubes with heat source and radiative effects

Muapper Alhadri [a], Tasawar Abbas [b], Sami Ullah Khan [c,*], Lotfi Ben Said [a], Walid Aich [a], Lioua Kolsi [a], Huma Tayyab [b]

a. Department of Mechanical Engineering, College of Engineering, University of Ha'il, Ha'il City, Saudi Arabia.
b. Department of Mathematics, University of Wah, Wah Cantt, Pakistan.
c. Department of Mathematics, Namal University, Mianwali, Pakistan.

* Corresponding author: samiullah@namal.edu.pk (S.U. Khan)

Received 22 November 2023; Received in revised form 4 September 2024; Accepted 2 December 2024

Keywords

Heat transfer;
Carbon Nanotubes (CNTs);
Ethylene Glycol (EG);
Rotating disk;
Slip effects.

Abstract

The objective of the current work is to characterize the thermal impact of Carbon Nanotubes (CNTs) due to a rotating disk, with applications of thermal radiation, heat source, and slip effects. Single-Walled Carbon Nano -Tubes (SWCNTs) and Multi-Walled Carbon Nano-Tubes (MWCNTs) with a suspension of Ethylene Glycol (EG) have been used to analyze the problem. The base fluid consequences are justified by using the Casson fluid. The flow model is justified by the interaction of velocity and thermal slip effects. Thermal characteristics of SWCNT and MWCNT along EG base materials have been presented. The heat transfer investigation is based on the implementation of the Cattaneo-Christov approach. Numerical computations are performed with the help of the shooting scheme. Comparative thermal analysis is performed for traditional nanofluid (SWCNT/EG) and hybrid nanofluid (SWCNTs-MWCNTs/EG). Physical visualization of results for the enhancement of the heat transfer phenomenon is performed. It has been observed that the heat transfer phenomenon is more pronounced for the hybrid nanofluid (SWCNTs-MWCNTs/EG) as compared to the nanofluid (SWCNT/EG). The thermal profile improves for the Casson fluid parameter.

1. Introduction

Hybrid nanomaterials are a modified class of nanofluids having efficient thermal properties. The hybrid nanofluid represents the joint suspension of two distinct nanoparticles with a base fluid. The interaction of two different nanoparticles shows stronger thermal performance as compared to common nanofluids. Owing to high thermal impact, the hybrid nanofluids offer various kinds of applications in refrigeration, nuclear systems, heat exchangers, chemical reactions, aircraft, thermal reservoirs, etc. Researchers have performed various investigations for studying the hybrid nanofluid thermal impact. For instance, Sundar et al. [1] focused on investigating the thermal interpretation of hybrid nanofluid under the influence of different friction sources. Ahmad et al. [2] addressed the heat transfer impact due to graphene oxide and silver nanoparticles in order to evaluate the boosted performance of kerosene oil-based liquid. Ali et al. [3] predicted the thermo-fluid aspects of a hybrid nanofluid due to a Couette channel. Faridi et al. [4] predicted the heat fluctuation of a hybrid nanofluid due to stretched surface flow. Analysis highlighting the thermal reservations of Carbon Nanotubes (CNTs) confined to a curved surface was elaborated by Abideen and Saif [5]. Mebarek-Oudina et al. [6] visualized the hydromagnetic flow of magnetite nanoparticles to improve the heat transfer phenomenon. Borode et al. [7] worked out artificial neural network analysis for describing the thermophysical

To cite this article:
M. Alhadri, T. Abbas, S.U. Khan, L. Ben Said, W. Aich, L. Kolsi, H. Tayyab "Thermal applications of hybrid nanofluid containing carbon nanotubes with heat source and radiative effects", *Scientia Iranica* (2025) **32**(18): 8476. https://doi.org/10.24200/sci.2024.63581.8476

properties of hybrid nanofluid via an experimental approach. Manjakuppam and Sonawane [8] deduced the thermal simulations based on hybrid nanofluid flow with significance to heat exchangers. Titanium oxide and silica nanoparticles were used to improve the thermal performance of water-based fluid. Alawi et al. [9] described solar collector applications due to the utilization of hybrid nanomaterials. The results were supported by machine learning algorithms. The squeezing flow of copper oxide and aluminum nanoparticles for Darcy-Forchheimer applications has been analyzed by Hayat et al. [10]. Acharya and Öztop [11] present an investigation of energy storage due to the semi-circular flow of hybrid nanofluid. Srilatha et al. [12] studied the machine learning analysis for the interface layer of hybrid nanofluid due to a porous disk. Foukhari et al. [13] performed an evaluation of entropy production due to a hybrid nanofluid due to two coaxial porous cylinders. Sarfaraz and Khan [14] claimed the heat transfer improvement with the interaction of a hybrid nanofluid in a wedge-shaped surface. Mehdi et al. [15] utilized the entropy generation effects in curved surface flow comprising the hybrid nanofluid. Rostami et al. [16] studied the thermal outcomes for dust particles with a mixture of hybrid nanofluid. Zangooee et al. [17] used the interference of slip to inspect the diverse thermal mechanisms of hybrid nanofluid. Hosseinzadeh et al. [18] performed the heat transfer computations based on iron oxide and molybdenum disulfide nanoparticles in a sinusoidal cylinder. Comparative thermal observations for the thermal evaluation associated with concave parabolic, trapezoidal, and convex cross configurations with utilization of hybrid nanofluid have been inspected by Hosseinzadeh et al. [19]. Paul et al. [20] depicted the contribution of a Casson hybrid nanofluid governed by an exponentially stretched cylinder. An investigation for improvement of heat fluctuation in vertically driven flow of hybrid nanofluid was proposed by Paul et al. [21]. Sarma and Paul [22] analyzed the bioconvective achievement for decomposition of hybrid nanoparticles. Copper oxide and gold nanoparticles were used to investigate the thermal phenomenon. The heat fluctuation due to ternary hybrid nanofluid in a rotating disk was visualized by Paul et al. [23]. In another investigation, Paul et al. [24] utilized the Hall effect in Casson hybrid nanofluid flow with fluctuation of heat transfer.

In the above-cited research work, it has been noticed that various studies have been performed to analyze the heat transfer due to hybrid nanofluid. However, comparative thermal observations for nanofluid and hybrid nanomaterial due to a rotating disk with slip effects have not been focused on yet. Therefore, the objective of the current work is to study comparative thermal analysis due to radiative flow of hybrid nanofluid with the application of slip effects and an external heat source. The hybrid nanofluid is based on the interaction of Single Walled Carbon Nano-Tubes (SWCNTs) and Multi-Walled Carbon Nano-Tubes (MWCNTs) with Ethylene Glycol (EG) base fluid. Comparative thermal simulations are presented for traditional nanofluid (SWCNTs/EG) and hybrid nanofluids (SWCNTs-MWCNTs/EG). The novel aspects of this investigation are:

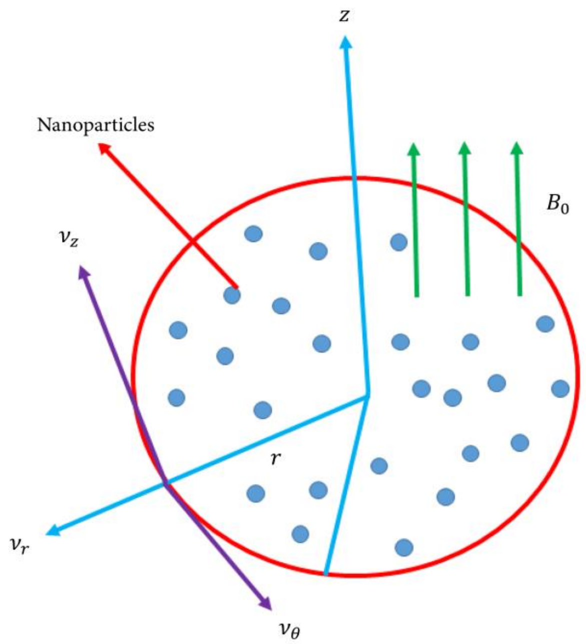

Figure 1. Illustration of the flow problem.

- A suspension of SWCNTs and MWCNTs with EG due to a rotating disk has been considered;
- The base fluid properties are highlighted by the Casson fluid model;
- The investigation is subject to velocity and thermal slip constraints;
- The heat transfer model is updated with the implementation of Cattaneo-Christov theory;
- Numerical computations associated with the flow problem are performed with a shooting scheme;
- Comparative analysis is performed for prediction of heat transfer for traditional nanofluid (SWCNTs/EG) and hybrid nanofluids (SWCNTs-MWCNTs/EG).

2. Formulation of the problem

Let us observe the heat transfer analysis due to the interaction of SWCNTs and MWCNTs with the EG base liquid. The flow problem is modeled in view of the following flow assumptions:

- Assuming a steady flow transport of Ethylene Glycol base fluid with a suspension of SWCNTs and MWCNTs.
- The rotatory disk accounts for the flow as shown in Figure 1.

- For development of mathematical model, the cylindrical coordinates are used with coordinates r, θ and z, Denoting velocity components with v_r, v_θ and v_z.
- The rotation of the disk is considered along the z-direction maintain angular velocity Ω.
- Slip effects for both temperature and velocity profiles have been considered [25].
- The heat source and radiation significance for the inspection of heat transfer are considered.
- The upgraded energy equation is used with the implication of the modified Fourier law.

The governing equations for the stated flow constraints are expressed as [5,25].

$$\frac{\partial v_r}{\partial r}+\frac{v_r}{r}+\frac{\partial v_z}{\partial z}=0, \tag{1}$$

$$\rho_{hnf}\left(v_r\frac{\partial v_r}{\partial r}+v_z\frac{\partial v_r}{\partial z}-\frac{{v_\theta}^2}{r}\right)=\mu_{hnf}\left(1+\frac{1}{\gamma}\right)\left(\frac{\partial^2 v_r}{\partial r^2}+\frac{1}{r}\frac{\partial v_r}{\partial r}+\frac{\partial^2 v_r}{\partial z^2}-\frac{v_r}{r^2}\right)-\sigma_{hnf}{B_0}^2 v_r, \tag{2}$$

$$\rho_{hnf}\left(v_r\frac{\partial v_\theta}{\partial r}+v_z\frac{\partial v_\theta}{\partial z}-\frac{v_r v_\theta}{r}\right)=\mu_{hnf}\left(1+\frac{1}{\gamma}\right)\left(\frac{\partial^2 v_\theta}{\partial r^2}+\frac{1}{r}\frac{\partial v_\theta}{\partial r}+\frac{\partial^2 v_\theta}{\partial z^2}-\frac{v_\theta}{r^2}\right)-\sigma_{hnf}{B_0}^2 v_\theta, \tag{3}$$

$$\rho_{hnf}\left(v_r\frac{\partial v_z}{\partial r}+v_z\frac{\partial v_z}{\partial z}\right)=\mu_{hnf}\left(1+\frac{1}{\gamma}\right)\left(\frac{\partial^2 v_z}{\partial r^2}+\frac{1}{r}\frac{\partial v_z}{\partial r}+\frac{\partial^2 v_z}{\partial z^2}\right), \tag{4}$$

with boundary conditions [2]; We have Eq. (5) is shown in Box I.

$$v_r=rs+L_0\left(1+\frac{1}{\gamma}\right)\frac{\partial v_r}{\partial z}, \qquad v_\theta=r\Omega+L_0\left(1+\frac{1}{\gamma}\right)\frac{\partial v_\theta}{\partial z},$$

$$v_z=0, T=T_w+N_0\frac{\partial T}{\partial z}, \quad \text{at} \quad z=0. \tag{6}$$

$$v_r\to 0, \quad v_\theta\to 0, \quad T\to T_\infty \quad \text{as} \quad z\to\infty. \tag{7}$$

With μ_{hnf} (dynamic viscosity of hybrid nanoparticles), T_w (surface temperature), γ (Casson fluid coefficient), B_0 (magnetic field strength), $(\rho C_p)_{hnf}$ (heat capacitance), T (fluid temperature), L_0 (velocity slip coefficient), N_0 (thermal slip coefficient), ρ_{hnf} (hybrid nanofluid density), λ_t (thermal relaxation time), σ^* (Stefan Boltzmann constant), T_∞ (free stream temperature), α_{hnf} (thermal diffusivity), Q_0 (external heat source coefficient), and k^* (absorption coefficient). Numerical values for various thermal properties of SWCNTs-MWCNTs/EG suspension have been expressed in Table 1.

Table 1. Thermal properties SWCNTs and MWCNTs with EG base liquid.

Physical properties	**Ethylene Glycol (WE)**	**SWCNT**	**MWCNT**
Density	1059.68	2600	1600
Specific heat	335257	425	796
Thermal conductivity	0.404	6600	3000
Electrical conductivity	0.00276	10^6-10^7	1.9×10^{-4}

To transform the problem into dimensionless form, the following similarity transformations are suggested [5,25]:

$$v_r=r\Omega f'(\zeta), \quad v_\theta=r\Omega h(\zeta), \quad v_z=-(2\Omega\upsilon_f)^{1/2} f(\zeta),$$

$$\theta(\zeta)=\frac{T-T_\infty}{T_w-T_\infty}, \qquad \zeta=z\left(\frac{2\Omega}{\nu_f}\right)^{1/2}. \tag{8}$$

The dimensionless form is:

$$2\left(1+\frac{1}{\gamma}\right)f'''-\zeta_1\left[f'^2-2ff''-h^2+\zeta_2 Mf'\right]=0, \tag{9}$$

$$2\left(1+\frac{1}{\gamma}\right)h''+\zeta_1\left[2fh'-2f\hbar-\zeta_3 Mh\right]=0, \tag{10}$$

$$(\zeta_4+Rd)\theta''+\Pr Q\theta+\zeta_2\Pr\left[f\theta'-\alpha\left(f^2\theta''+ff'\theta'\right)\right]=0, \tag{11}$$

and the boundary conditions are given below:

$$f(0)=0, \quad f'(0)=A+\left(1+\frac{1}{\gamma}\right)\delta f''(0),$$

$$h(0)=1+\left(1+\frac{1}{\gamma}\right)\delta f'(0), \tag{12}$$

$$\theta(0)=1+\beta\theta'(0), \quad f'(\infty)=h(\infty)=\theta(\infty)\to 0. \tag{13}$$

where M (Hartmann constant), Pr (Prandtl constant), α (thermal relaxation coefficient), A (stretching constant), δ (velocity slip parameter) and β (thermal slip parameter), Rd (thermal radiation) and Q (heat generation) which are defined

$$v_r\frac{\partial T}{\partial r}+v_z\frac{\partial T}{\partial z}=\alpha_{hnf}\left(\frac{\partial^2 T}{\partial r^2}+\frac{1}{r}\frac{\partial T}{\partial r}+\frac{\partial^2 T}{\partial z^2}\right)-\frac{16}{3}\frac{\sigma^* {T_\infty}^3}{k^*(\rho c_p)_{hnf}}\left(\frac{\partial^2 T}{\partial r^2}+\frac{1}{r}\frac{\partial T}{\partial r}+\frac{\partial^2 T}{\partial z^2}\right)$$
$$-\lambda_t\left[{v_r}^2\frac{\partial^2 T}{\partial r^2}+{v_z}^2\frac{\partial^2 T}{\partial z^2}+2v_r v_z\frac{\partial^2 T}{\partial r\partial z}+\left(v_r\frac{\partial v_r}{\partial r}+v_z\frac{\partial v_r}{\partial z}\right)\frac{\partial T}{\partial r}+\left(v_r\frac{\partial v_z}{\partial r}+v_z\frac{\partial v_z}{\partial z}\right)\frac{\partial T}{\partial z}\right]-\frac{Q_0}{(\rho c_p)_{hnf}}(T-T_\infty), \tag{5}$$

Box I

Table 2. Thermo-physical features of nanofluid (SWCNTs/EG) and hybrid nanofluids (SWCNTs-MWCNTs/WE) [5].

Properties	**Hybrid nanofluid (SWCNT-MWCNT/WE)**	**Nanofluid (SWCNT/WE)**
Electrical conductivity	$\frac{\sigma_{hnf}}{\sigma_f}=\frac{\sigma_{SWCNT}-2\phi_{SWCNT}\left(\sigma_{nf}-\sigma_{SWCNT}\right)+2\sigma_{nf}}{\sigma_{SWCNT}+\phi_{SWCNT}\left(\sigma_{nf}-\sigma_{SWCNT}\right)+2\sigma_{nf}}$ $\frac{\sigma_{nf}}{\sigma_f}=\frac{\sigma_{MWCNT}-2\phi_{SWCNT}\left(\sigma_f-\sigma_{MWCNT}\right)+2\sigma_f}{\sigma_{MWCNT}+\phi_{MWCNT}\left(\sigma_f-\sigma_{MWCNT}\right)+2\sigma_f}$	$\frac{\sigma_{nf}}{\sigma_f}=1+\frac{3(\sigma-1)\phi}{(\sigma+2)-(\sigma-1)\phi}$ $\frac{\sigma_s}{\sigma_f}=\sigma$
Viscosity	$\mu_{hnf}=\frac{\mu_f}{\left(1-\phi_{SWCNT}\right)^{2.5}\left(1-\phi_{MWCNT}\right)^{2.5}}$	$\mu_{nf}=\frac{\mu_f}{(1-\phi)^{2.5}}$
Heat capacity	$\left(\rho C_p\right)_{hnf}=\left(\rho C_p\right)_f\left(1-\phi_{SWCNT}\right)\begin{bmatrix}\left(1-\phi_{MWCNT}\right)\\+\phi_{MWCNT}\frac{\left(\rho C_p\right)_{MWCNT}}{\left(\rho C_p\right)_f}\end{bmatrix}+\phi_{SWCNT}\left(\rho C_p\right)_{SWCNTs}$	$\left(\rho C_p\right)_{nf}=\left(\rho C_p\right)_f(1-\phi)+\phi\frac{\left(\rho C_p\right)_s}{\left(\rho C_p\right)_f}$
Density	$\rho_{hnf}=\rho_{SWCNT}\phi_{SWCNT}+\left[\left(1-\phi_{SWCNT}\right)\begin{Bmatrix}\left(1-\rho_{MWCNT}\right)\rho_f\\+\rho_{MWCNT}\phi_{MWCNT}\end{Bmatrix}\right]$	$\rho_{nf}=\rho_s\phi+(1-\phi)\rho_f$
Thermal conductivity	$\frac{k_{hnf}}{k_f}=\frac{\left(k_{SWCNT}+(n-1)k_{nf}\right)-(n-1)\phi_{SWCNT}\left(k_{nf}-k_{SWCNT}\right)}{\left(k_{SWCNT}+(n-1)k_{hnf}\right)+\phi_{SWCNT}\left(k_{nf}-k_{SWCNT}\right)}$	$\frac{k_{nf}}{k_f}=\frac{\left(k_s+(n-1)k_f\right)-\phi\left(k_f-k_s\right)}{\left(k_s+(n-1)k_f\right)+\phi\left(k_f-k_s\right)}$

as: $M=\sigma_f\frac{B_0{}^2}{\rho_f}\Omega$, $\Pr=\frac{\nu_f}{\alpha_f}$ $\alpha=2\lambda_t\Omega,$

$A=\frac{s}{\Omega}$, $\delta=L_0\left(\frac{2\Omega}{\nu_f}\right)^{1/2}$, $\beta=N_0\left(\frac{2\Omega}{\nu_f}\right)^{1/2}$,

$Rd=\frac{4}{3}\frac{\sigma^* T_\infty{}^3}{k^* k_f}$, $Q=\frac{Q_0}{\left(\rho c_p\right)_{hnf}}$.

Thermo-physical constants involved in the transformed equations are defined as:

$$\zeta_1=(1-\phi 1)^{2.5}(1-\phi 2)^{2.5}\left[(1-\phi 2)\left\{(1-\phi 1)+\phi 1\frac{\rho_{s1}}{\rho_f}\right\}+\phi 2\frac{\rho_{s2}}{\rho_f}\right], \quad (14)$$

$$\zeta_2=(1-\phi 1)^{2.5}(1-\phi 2)^{2.5}\frac{\sigma_{hnf}}{\sigma_f}, \quad (15)$$

$$\zeta_3=\left[(1-\phi 2)\left\{(1-\phi 1)+\phi 1\frac{\left(\rho c_p\right)_{s1}}{\left(\rho c_p\right)_f}\right\}+\phi 2\frac{\left(\rho c_p\right)_{s2}}{\left(\rho c_p\right)_f}\right], \quad (16)$$

$$\zeta_4=\frac{k_{hnf}}{k_f}=\left[\frac{\left(k_{s2}+2k_{nf}\right)-2\phi 1\left(k_{nf}-2k_{s2}\right)}{\left(k_{s2}+2k_{nf}\right)+\phi 1\left(k_{nf}-2k_{s2}\right)}\right]$$

$$\times\left[\frac{\left(k_{s1}+2k_f\right)-2\phi 2\left(k_f-k_{s1}\right)}{\left(k_{s1}+2k_f\right)+\phi 2\left(k_f-k_{s1}\right)}\right]. \quad (17)$$

Where $\phi 1$ defines the solid volume fractions of SWCNTs while $\phi 2$ be the volume fractions of MWCNTs. The mathematical expressions for hybrid nanofluid (SWCNTs-MWCNTs/EG) and nanofluid (SWCNTs/EG) are presented in Table 2.

Physical quantities skin friction and Nusselt number are defined by:

$$C_f=\frac{\tau_w}{\rho(\Omega r)^2}, \quad \tau_w=\mu_{hnf}\left(\frac{\partial u}{\partial y}\right)_{z=0},$$
$$Nu_x=\frac{rq_w}{k_f\left(T_w-T_\infty\right)}, \quad q_w=-k_{hnf}\left(\frac{\partial T}{\partial r}\right)_{z=0}, \quad (18)$$

$$\left(\mathrm{Re}_r\right)^{1/2}C_f=\frac{\left(1+\frac{1}{r}\right)}{\left(1-\phi_1\right)^{2.5}\left(1-\phi_2\right)^{2.5}}f''(0), \quad (19)$$

$$\left(\mathrm{Re}_r\right)^{-1/2}Nu_r=-\left(\frac{k_{hnf}}{k_f}\right)\theta'(0). \quad (20)$$

Where $\mathrm{Re}_r=\frac{(\Omega r)r}{\upsilon_f}$ is the local Reynolds number.

Table 3. Comparison of numerical results with the study of Mustafa [26] taking A=0, $\phi_1 = \phi_2 = 1$ and $\gamma \rightarrow \infty$.

Parameters		Mustafa [26]		Present results	
M	δ	$f'(0)$	$f''(0)$	$f'(0)$	$f''(0)$
0.0	0.25	0.064883	0.259534	0.064885	0.259535
0.2	0.25	0.047794	0.191176	0.047795	0.191177
0.4	0.25	0.036514	0.146057	0.036513	0.146056

3. Numerical computations

This section incorporates the implementation of the shooting scheme for a set of modeled equations. To initiate the simulations, the higher-order system is first converted into a first-order system with the help of following transformations:

$$(s_1, s_2, s_3, s_4, s_5, s_6, s_7) = (f, f', f'', h, h', \theta, \theta'), \tag{21}$$

$$\begin{pmatrix} s_1' \\ s_2' \\ s_3' \\ s_4' \\ s_5' \\ s_6' \\ s_7' \end{pmatrix} = \begin{pmatrix} s_2 \\ s \\ \dfrac{\zeta_1 \left(s_2^2 - 2s_1 s_3 - s_4^2 + \zeta_2 M s_2\right)}{2\left(1+\frac{1}{r}\right)} \\ S_5 \\ \dfrac{-\zeta_1}{2\left(1+\frac{1}{r}\right)}\left[2s_1 s_5 - 2s_2 s_4 - \zeta_2 M s_4\right] \\ S_7 \\ \dfrac{1}{\left((\zeta_4 + Rd) - \Pr \alpha s_1^2\right)}\left[\zeta_3 \Pr s_1 s_7 (\alpha s_2 - 1) - \Pr Q s_6\right] \end{pmatrix} \tag{22}$$

The boundary conditions are reduced to:

$$\begin{pmatrix} s_1(0) \\ s_2(0) \\ s_3(0) \\ s_4(0) \\ s_5(0) \\ s_6(0) \\ s_7(0) \end{pmatrix} = \begin{pmatrix} 0 \\ A + \left(1+\frac{1}{r}\right)\delta s_1 \\ s_1 \\ 1 + \left(1+\frac{1}{r}\right)\delta s_2(0) \\ s_2 \\ 1+\beta s_3 \\ s_4 \end{pmatrix}. \tag{23}$$

4. Validation of results

The simulated numerical data have been confirmed by comparison with the investigation of Mustafa [26]. Table 3 shows that the current numerical results claim fine accuracy compared with Mustafa [26].

5. Results and discussion

Physical interpretation of results has been visualized in this section. Comparative results are prepared for both nanofluid (SWCNTs/EG) and hybrid nanofluids (SWCNTs MWCNTs/EG) with variation of modeled parameters. Figure 2 interprets the contribution of stretching constant A on radial velocity f'.

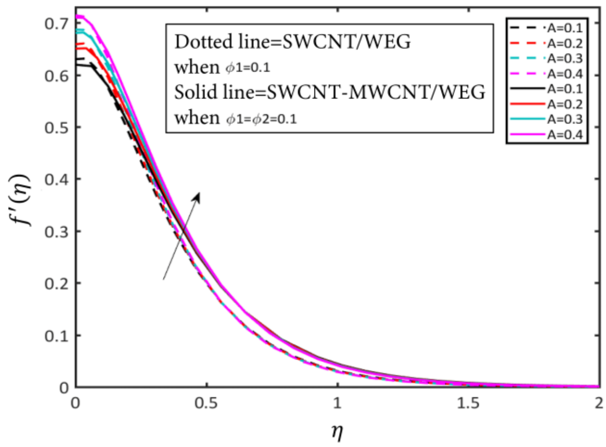

Figure 2. Velocity profile f' for A.

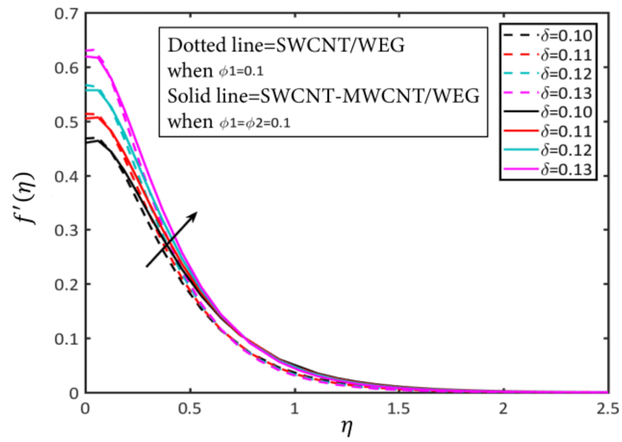

Figure 3. Velocity profile f' for δ.

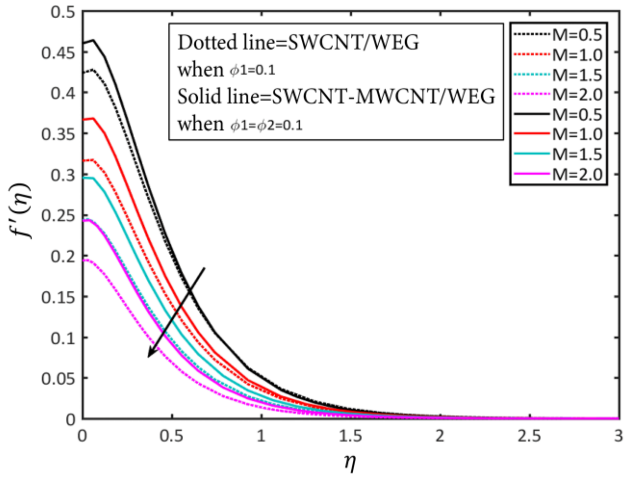

Figure 4. Velocity profile f' for M.

arising numeric values, the radial velocity increases for both fluids. The enhancement in f' is more prominent for SWCNTs-MWCNTs/EG decomposition. Figure 3 helps to visualize the significance of the velocity slip parameter δ on f' for both SWCNTs/EG and SWCNTs-MWCNTs/EG suspensions. Leading values of δ slow down the velocity for both decompositions. The momentum boundary layer also becomes thinner with increasing variation of δ. The physical description discussed in Figure 4 shows the truncated profile of f' upon increasing Hartmann number M.

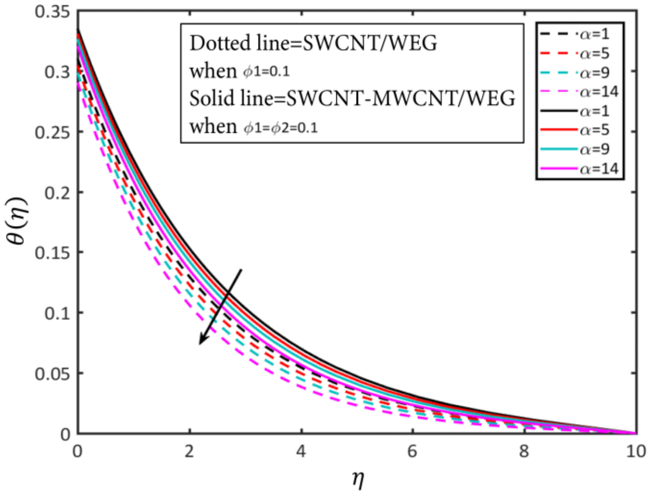

Figure 5. Temperature profile θ for α .

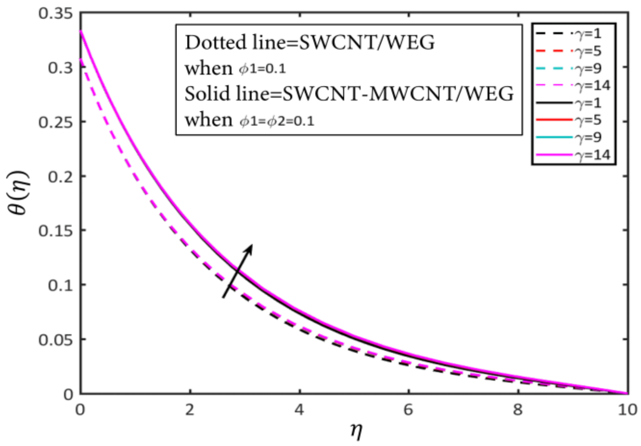

Figure 6. Temperature profile θ for γ .

The velocity profile gets compressed due to *M*. Physically, peak values of *M* lead to the interpretation of the Lorentz force, which slows down the velocity. Furthermore, a low velocity profile is more progressive for SWCNTs/EG suspension.

Figure 5 explains the role of the thermal relaxation factor α on the temperature profile θ. The temperature field decreases for prominent values of α. The thermal observations are deduced by varying α for SWCNTs-MWCNTs/EG and SWCNTs/EG decomposition. Physically, higher values of α are associated with the time required for the fluid to maintain its original position. The reduction in θ is pronounced for SWCNTs-MWCNTs/EG. The results for observations of the thermal profile due to the Casson fluid parameter γ have been predicted in Figure 6.

The temperature profile θ increases due to γ. However, the magnitude of the enhancement of θ is slower. Moreover, the heat transfer improvement is superior for the hybrid nanofluid (SWCNTs-MWCNTs/EG).

Figure 7 presents comparative results for heat transfer subject to Casson fluid (Q_1=Q_2=0), SWCNTs/EG. (Q_1=0.1 Q_2=0) (MWCNTs/EG (Q_1=0, Q_2=0.1) and SWCNTs-MWCNTs/EG (Q_1=Q_2= 0.1).

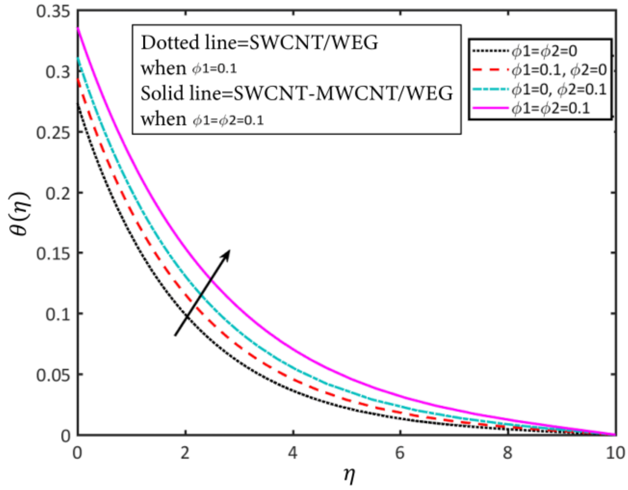

Figure 7. Temperature profile θ for Casson fluid, Casson nano-fluid and Casson hybrid nanofluid.

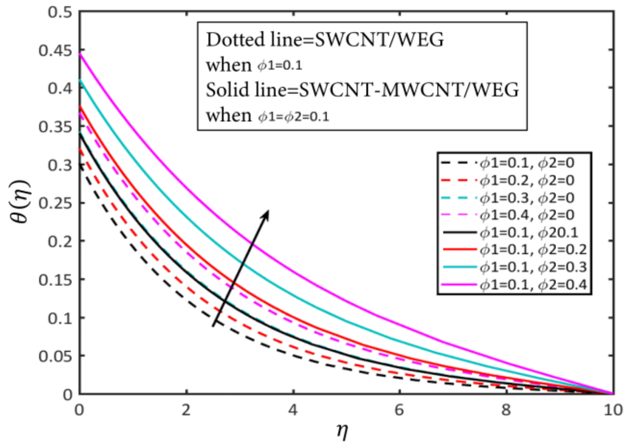

Figure 8. Temperature profile θ for $\phi_1 = 0.1,\ \phi_2 = 0$

Heat transfer fluctuation is slower for the Casson fluid, while improved results for the thermal profile are associated (Q_1= Q_2=0.1). Figure 8 aims to understand the behavior of θ in view of the nanoparticles volume fraction Q_1 and Q_2. Comparative observations are revealed for SWCNTs/ EG and SWCNTs-MWCNTs/EG. The figure clearly indicates that θ is enriched with variation of Q_1 and Q_2. The improvement in heat transfer is maximum for SWCNTs-MWCNTs/EG as compared to SWCNTs /EG. In Figure 9, the results for the influence of Prandtl number Pr are shown against θ. A larger change in Pr pronounced lower heat transfer for nanofluid and hybrid nanofluid. Physically, larger values of Pr correspond to low mass diffusivity, due to which θ shows retarded trend. In order to evaluate the performance of heat source Q on θ, Figure 10 has been prepared.

An increasing variation with larger Q is exhibited in the profile of θ. The presence of a heat source provides extra energy to the system, which boosts the temperature profile. Figure 11 reflects the analysis for the radiation parameter *Rd* on θ.

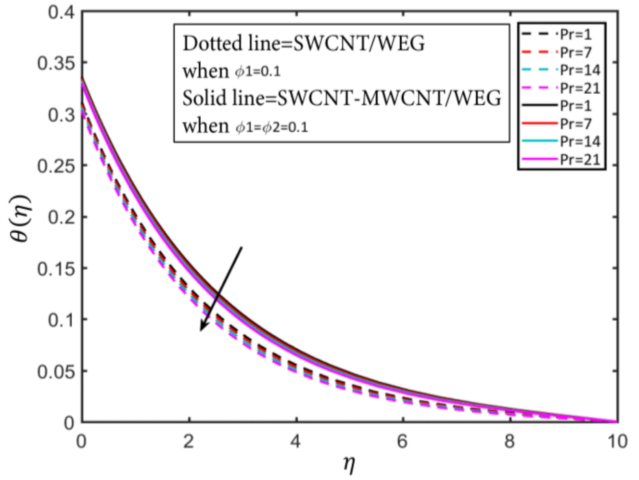

Figure 9. Temperature profile θ for Pr.

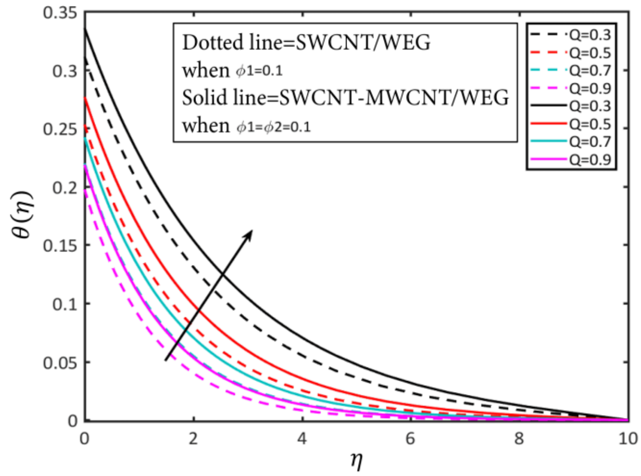

Figure 10. Temperature profile θ for Q.

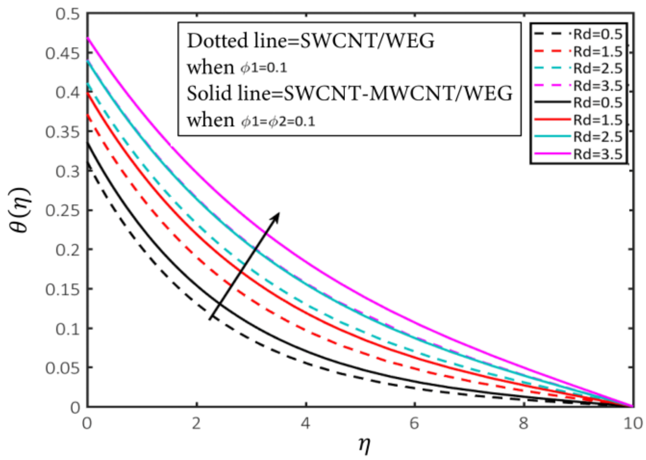

Figure 11. Temperature profile θ for *Rd*.

Change in *Rd* leads to a boost in the temperature profile for both SWCNTs-MWCNTs/EG and SWCNTs/EG. The radiation phenomenon is associated with the transfer of energy through electromagnetic waves.

6. Conclusion

The heat transfer analysis with the utilization of Single-Walled (SW) and Multi-Walled (MW) carbon nanofluid with Ethylene Glycol (EG) base fluid has been performed for a rotating disk. The significance of heat and radiative phenomena is addressed. The Cattaneo-Christov heat flux model is used to modify the heat equation. Comparative thermal observations for nanofluid Single-Walled Carbon Nano-Tubes/Ethylene Glycol (SWCNTs/EG) and hybrid nanofluid (SWCNTs-MWCNTs/EG) are investigated. The major results are summarized as:

- The radial velocity increases due to the stretching parameter for the nanofluid and hybrid nanofluid. However, the interaction of slip leads to a reduction in the velocity profile.
- A change in the thermal relaxation parameter leads to a decrement in the temperature profile for both SWCNTs/EG and SWCNTs-MWCNTs/EG suspensions.
- Heat transfer is enhanced for the Casson fluid parameter. The improvement in the thermal profile is prominent for the hybrid nanofluid.
- The fluctuation in heat transfer is more pronounced for the hybrid nanofluid as compared to the traditional nanofluid.
- Subject to increasing heat source and radiation parameter, the temperature profile increased.
- The heat transfer phenomenon increases for the nanoparticles' volume fraction of Single-Walled Carbon SWCNTs and Multi-Walled Carbon Nanotubes (MWCNTs). However, the improvement in thermal profile is dominant for MWCNTs.
- The modification in the current results can be suggested by studying the entropy generation analysis, bioconvection phenomenon and stability analysis.

Acknowledgment

This research has been funded by the Scientific Research Deanship at the University of Ha'il, Saudi Arabia, through project number RG-24 028.

Authors contribution statement

First author: Data curation; Formal analysis;
Second author: Methodology; Resources; Software;
Third author: Conceptualization; Data curation;
Fourth author: Formal analysis;
Fifth author: Investigation;
Sixth author: Project administration; Visualization;
Seventh author: Writing - original draft; Writing - review and editing.

References

1. Sundar, L.S., Sharma, K.V., Singh, M.K., et al. "Hybrid nanofluids preparation, thermal properties, heat transfer and friction factor –A review," *Renew. Sustain. Energy Rev.*, **68**, pp. 185–198 (2017). https://doi.org/10.1016/j.rser.2016.09.108

2. Ahmad, F., Abdal, S., Ayed, H., et al. "The improved thermal efficiency of Maxwell hybrid nanofluid comprising of graphene oxide plus silver /kerosene oil over stretching sheet", *Case Stud Therm. Eng.* **27**, 101257 (2021). https://doi.org/10.1016/j.csite.2021.101257

3. Ali, K., Reddy, Y.R., and Shekar, B.C. "Thermo-fluidic transport process in magnetohydrodynamic Couette channel containing hybrid nanofluid", *Partial Diff. Eqs. Appl. Math.* **7,** 100468 (2023). https://doi.org/10.1016/j.padiff.2022.100468

4. Faridi, A.A., Khan, N., and Ali, K. "A novel numerical note on the enhanced thermal features of water-ethylene glycol mixture due to hybrid nanoparticles ($MnZnFe_2O_4$-Ag) over a magnetized stretching surface", *Numer. Heat Transf. B.*, pp. 1–23 (2023). https://doi.org/10.1080/10407790.2023.2296082

5. Abideen, Z.U. and Saif, R.S. "Impact of thermal radiation and internal heat generation on Casson nano-fluid flowing by a curved stretchable surface with suspension of carbon nanotubes (CNTs)", *Heliyon*, **9**(8), e18941 (2023). https://doi.org/10.1016/j.heliyon.2023.e18941

6. Mebarek-Oudina, F., Preeti, A.S. Sabu et al. "Hydromagnetic flow of magnetite–water nanofluid utilizing adapted Buongiorno model", *Int. J. Modern Phys. B.,* **38**(01), 2450003 (2024). https://doi.org/10.1142/S0217979224500036

7. Borode, A., Tshephe, T., Olubambi, P., et al. "Effects of temperature and nanoparticle mixing ratio on the thermophysical properties of GNP–Fe_2O_3 hybrid nanofluids: an experimental study with RSM and ANN modeling", *J. Therm. Anal. Calor.*, **149**, pp. 5059-5083 (2024). https://doi.org/10.1007/s10973-024-13029-3

8. Manjakuppam, M. and Sonawane, S.S. "Ecological optimization and LCA of TiO_2-SiC/water hybrid nanofluid in a shell and tube heat exchanger by ANN", *Proc. Inst. Mech. Eng. E.,* **238**(1), pp. 45-55 (2024). https://doi.org/10.1177/09544089221093304

9. Alawi, O.A., Kamar, H.M., Ali, H., et al. "Design optimization of solar collectors with hybrid nanofluids: An integrated ansys and machine learning study", *Solar Energy Materials and Solar Cells*, **271**, 112822 (2024). https://doi.org/10.1016/j.solmat.2024.112822

10. Hayat, T., Fatima, A., and Muhammad, K. "Heat transfer and entropy analysis in squeezing flow of hybrid nanofluid (Au-CuO/NaAlg) with DF (Darcy-Forchheimer) and CC (Cattaneo-Christov) heat flux", *Mater. Sci. Eng. B*, 288, 116150 (2023). https://doi.org/10.1016/j.mseb.2022.116150

11. Acharya, N. and Öztop, H.F. "On the entropy analysis and hydrothermal behavior of buoyancy-driven magnetized hybrid nanofluid flow within a semi-circular chamber fitted with a triangular heater: application to thermal energy storage for energy management", *Numer. Heat Transf. A.,* pp. 1-31 (2023). https://doi.org/10.1080/10407782.2023.2281541

12. Srilatha, P., Gowda, R.J.P., Madhu, J., et al. "Designing a solid–fluid interface layer and artificial neural network in a nanofluid flow due to rotating rough and porous disk", *J. Therm. Anal. Calor.,* **149**(2), pp. 867-878 (2024). https://doi.org/10.1007/s10973-023-12706-z

13. Foukhari, Y., Sammouda, M., and Driouich, M. "Entropy generation analysis of hybrid-nanofluid during natural convection through two coaxial cylinders partially filled with porous medium under magnetic field", *Scientia Iranica* (2024). https://doi.org/10.24200/sci.2024.62997.8159

14. Sarfaraz, M. and Khan, M. "Energy optimization of water-based hybrid nanomaterials over a wedge-shaped channel", *Sci. Iran.* **31**(1), pp. 71-82 (2024). https://doi.org/10.24200/sci.2023.60254.6689

15. Mehdi, M., Hosseinzadeh, Kh., and Ganji, D.D., "Entropy generation analysis and hydrothermal optimization of ternary hybrid nanofluid flow suspended in polymer over curved stretching surface", *Int. J. Thermofluids*, **20**, 100507 (2023). https://doi.org/10.1016/j.ijft.2023.100507

16. Rostami, T., Najafabadi, H.M.F., Hosseinzadeh, Kh., et al. "Investigation of mixture-based dusty hybrid nanofluid flow in porous media affected by magnetic field using RBF method", *Int. J. Amb. Energy,* **43**(1), pp. 6425-6435 (2022). https://doi.org/10.1080/01430750.2021.2023041

17. Zangooee, M.R., Hosseinzadeh, Kh., and Ganji, D.D. "Hydrothermal analysis of hybrid nanofluid flow on a vertical plate by considering slip condition", *Theor. Appl. Mech. Lett.,***12**(5), 100357 (2022). https://doi.org/10.1016/j.taml.2022.100357

18. Hosseinzadeh, Kh., Mardani, M.R., Salehi, S., et al. "Investigation of micropolar hybrid nanofluid (iron oxide–molybdenum disulfide) flow across a sinusoidal cylinder in presence of magnetic field", *Int. J. Appl. Comput. Math.* **7**, pp. 1-17 (2021). https://doi.org/10.1007/s40819-021-01148-6

19. Hosseinzadeh, S., Hosseinzadeh, Kh., Hasibi, A., et al. "Thermal analysis of moving porous fin wetted by hybrid nanofluid with trapezoidal, concave parabolic and convex cross sections", *Case Stud. Therm. Eng.* **30**, 101757 (2022). https://doi.org/10.1016/j.csite.2022.101757

20. Paul, A., Das, T.K., and Nath, J.M. "Numerical investigation on the thermal transportation of MHD Cu/Al_2O_3-H_2O Casson-hybrid-nanofluid flow across an exponentially stretching cylinder incorporating heat source", *Phys. Scr.* **97**(8), 085701 (2022).

https://doi.org/10.1088/1402-4896/ac7981

21. Paul, A., Das, T.K., and Nath, J.M. "Thermally stratified Cu–Al_2O_3/water hybrid nanofluid flow with the impact of an inclined magnetic field, viscous dissipation and heat source/sink across a vertically stretching cylinder", *Zeitschrift für Angewandte Mathematik und Mechanik,* **104**(2), e202300084 (2024). https://doi.org/10.1002/zamm.202300084

22. Sarma, N. and Paul, A. "Thermophoresis and Brownian motion influenced bioconvective cylindrical shaped Ag–cuo/H_2O ellis hybrid nanofluid flow along a radiative stretched tube with inclined magnetic field", *BioNanoScience*, **14**(2), pp. 1266-1292 (2024). https://doi.org/10.1007/s12668-023-01280-1

23. Paul, A., Patgiri, B., and Sarma, N. "Darcy-Forchheimer flow of Ag–ZnO–$CoFe_2O_4$/H_2O Casson ternary hybrid nanofluid induced by a rotatory disk with EMHD", *Int. J. Amb. Energy*, **45**(1), e2313697 (2024). https://doi.org/10.1080/01430750.2024.2313697

24. Paul, A., Patgiri, B., and Sarma, N. "Transformer oil-based Casson ternary hybrid nanofluid flow configured by a porous rotating disk with Hall current, *Zeitschrift für Angewandte Mathematik und Mechanik,* **104**(4), e202300704 (2024). https://doi.org/10.1002/zamm.202300704

25. Puneet R., Mackolil, J., Mahanthesh, B., and Muhammad, T. "Cattaneo-Christov Theory to model heat flux effect on nanoliquid slip flow over a spinning disk with nanoparticle aggregation and Hall current", *Waves in Random and Complex Media*, **35**(2), pp. 2915-2937 (2022). DOI: 10.1080/17455030.2022.2048127

26. Mustafa, M. "MHD nanofluid flow over a rotating disk with partial slip effects: Buongiorno model", *Int. J. Heat Mass Tran.* **108**, pp. 1910–1916 (2017). https://doi.org/10.1016/j.ijheatmasstransfer.2017.01.064

Biographies

Muapper Alhadri is an Associate Professor at the University of Ha'il, Ha'il City, Saudi Arabia. He has received a PhD degree in Mechanical Engineering. His research expertise is in Fluid Mechanics and Numerical Analysis.

Tasawar Abbas is working at the University of Wah, Wah Cantt, Pakistan. His area of research is fluid mechanics and nanofluids.

Sami Ullah Khan is an Associate Professor at Namal University, Mianwali, Pakistan.

Lotfi Ben Said is an Associate Professor at the University of Ha'il, Ha'il City, Saudi Arabia. He has received a PhD degree in Mechanical Engineering. His research expertise is in Mechanical and Manufacturing Engineering.

Walid Aich is a professor at the University of Hail, Saudi Arabia. He is working in Thermal Systems and Numerical Analysis.

Lioua Kolsi is an Associate Professor at the University of Hail, Saudi Arabia. He is working in Thermal Systems. His area of research is nanofluids, thermal engineering, and computational fluid mechanics.

Huma Tayyab is working as a lecturer in the Department of Mathematics, University of Wah, Wah Cantt, Pakistan. She completed her MSc in computational fluid mechanics in 2022. Her area of research is fluid mechanics and nanotechnology.